JOURNAL OF BACTERIOLOGY, Dec. 2006, p. 8178–8188 Vol. 188, No. 23
0021-9193/06/$08.00+0 doi:10.1128/JB.01006-06

Global Map of Growth-Regulated Gene Expression in *Burkholderia pseudomallei*, the Causative Agent of Melioidosis▽

Fiona Rodrigues,[1] Mitali Sarkar-Tyson,[2] Sarah V. Harding,[2] Siew Hoon Sim,[3] Hui Hoon Chua,[1] Chi Ho Lin,[1] Xu Han,[1] R. Krishna M. Karuturi,[1] Ken Sung,[1] Kun Yu,[5] Wei Chen,[4] Timothy P. Atkins,[2] Richard W. Titball,[2] and Patrick Tan[1,4]*

Genome Institute of Singapore, 60 Biopolis Street, no. 02-01, Genome, Singapore 138672, Republic of Singapore[1]; Defence Science and Technology Laboratory, Porton Down, Salisbury, Wiltshire SP4 OJQ, United Kingdom[2]; Defence Medical and Environmental Research Institute, DSO National Laboratories, 27 Medical Drive, no. 13-14, Singapore 117510, Republic of Singapore[3]; and Agenica Research[4] and National Cancer Centre,[5] 11 Hospital Drive, Singapore 169610, Republic of Singapore

Received 9 July 2006/Accepted 13 September 2006

Many microbial pathogens express specific virulence traits at distinct growth phases. To understand the molecular pathways linking bacterial growth to pathogenicity, we have characterized the growth transcriptome of *Burkholderia pseudomallei*, the causative agent of melioidosis. Using a fine-scale sampling approach, we found approximately 17% of all *B. pseudomallei* genes displaying regulated expression during growth in rich medium, occurring as broad waves of functionally coherent gene expression tightly associated with distinct growth phases and transition points. We observed regulation of virulence genes across all growth phases and identified *serC* as a potentially new virulence factor by virtue of its coexpression with other early-phase virulence genes. *serC*-disrupted *B. pseudomallei* strains were serine auxotrophs and in mouse infection assays exhibited a dramatic attenuation of virulence compared to wild-type *B. pseudomallei*. Immunization of mice with *serC*-disrupted *B. pseudomallei* also conferred protection against subsequent challenges with different wild-type *B. pseudomallei* strains. At a genomic level, early-phase genes were preferentially localized on chromosome 1, while stationary-phase genes were significantly biased towards chromosome 2. We detected a significant level of chromosomally clustered gene expression, allowing us to predict ~100 potential operons in the *B. pseudomallei* genome. We computationally and experimentally validated these operons by showing that genes in these regions are preferentially transcribed in the same 5′→3′ direction, possess significantly shorter intergenic lengths than the overall genome, and are expressed as a common mRNA transcript. The availability of this transcriptome map provides an important resource for understanding the transcriptional architecture of *B. pseudomallei*.

Microbial growth is a conserved biological process that has been optimized by many bacteria to exploit environmental resources and ensure species survival. Under defined laboratory conditions, microbes undergo a series of predictable growth phases: (i) early phase, where the population density is low and nutrients are abundant (ii) log phase, where the population undergoes exponential expansion; and (iii) stationary phase, where the population density is high and nutrients are either absent or scarce. Recently, it has been shown that several pathogens appear to express important virulence traits at specific growth points, suggesting the presence of an intimate functional relationship between microbial growth and virulence. For example, the ability of *Pseudomonas aeruginosa* and *Salmonella enterica* serovar Typhimurium to invade and cause apoptosis in host cells is correlated with the entry of these microbes into stationary phase (12, 21), and many virulence genes in *Legionella pneumophila* are expressed at the transition from log phase to stationary phase (3). In general, most of these previous reports have focused primarily on characterizing genes expressed during stationary phase or the transition from log to stationary phase (20, 39, 48), and thus the potential contribution to virulence of genes expressed at other times, such as early phase, has been relatively unexplored. Previous studies have also typically analyzed only a limited number of samples representing each growth phase (16, 25, 40, 43). Studies with other systems, however, have shown that fine-scale sampling strategies can often improve upon the resolution of information that is broadly provided by coarser sampling approaches (4, 28).

The gram-negative pathogen *Burkholderia pseudomallei* is the causative agent of melioidosis, a serious, often fatal disease of both humans and animals and a recognized category B biowarfare agent (6). While *B. pseudomallei* is considered endemic to southeast Asia and northern Australia, recent melioidosis outbreaks in Brazil and Taiwan (15, 34) suggest that the geographical prevalence of *B. pseudomallei* may be increasing, making its study more crucial. The 7.2-Mb *B. pseudomallei* K96243 genome has been recently described and comprises two large circular chromosomes (chromosome 1 [Chr 1] and Chr 2) with >5,700 predicted genes, a number comparable to

* Corresponding author. Mailing address: Genome Institute of Singapore, 60 Biopolis Street, no. 02-01, Genome, Singapore 138672, Republic of Singapore. Phone: 65-6-478-8000. Fax: 65-6-478-9003. E-mail: tanbop@gis.a-star.edu.sg.
▽ Published ahead of print on 22 September 2006.

that for the eukaryotic model organism *Schizosaccharomyces pombe* (14). In this study, we describe a fine-scale transcriptomic characterization of growth-regulated gene expression in *B. pseudomallei*. We found that 17% of the *B. pseudomallei* genome is transcriptionally regulated during growth, taking the form of distinct gene expression cascades that were both functionally coherent and tightly associated with distinct growth phases and transition points. An analysis of these data allowed us to identify and experimentally validate *serC*, an early-phase gene, as a novel *B. pseudomallei* virulence factor. Furthermore, prior vaccination of mice with *serC* mutant *B. pseudomallei* conferred protection against subsequent challenges by different wild-type *B. pseudomallei* strains. When analyzed in a chromosomal context, we found that early-phase genes were preferentially localized towards chromosome 1, while stationary-phase genes were biased towards chromosome 2. Finally, the gene coexpression data allowed us to identify and map putative *B. pseudomallei* operons on a genome-wide scale. To our knowledge, this is the first report describing growth-regulated gene expression on a genome-wide scale for any member of the *Burkholderia* genus. As many of the genes in *B. pseudomallei* are evolutionarily conserved, our results are likely to find applicability and relevance to other microbial pathogens as well.

MATERIALS AND METHODS

Bacterial strains and media. *B. pseudomallei* strains K96243 and 576 are both clinical isolates from Thailand. *B. pseudomallei* 576 was provided by Ty Pitt, Central Public Health Laboratory, Clindale, United Kingdom. Strains were cultured at 37°C on rich medium (Luria Broth [LB] or tryptone soy broth [TSB]) or minimal medium (CDM) [10× stock: 0.03 M NaCl, 0.032 M $Mg_2SO_4 \cdot 7H_2O$, 0.03 M KCl, 0.03 M $(NH_4)_2SO_4$, 0.012 M K_2HPO_4, 0.55 M glucose, 0.5 M MOPS (morpholinepropanesulfonic acid)] lacking or supplemented with 15 mM L-serine.

***B. pseudomallei* growth curves.** Independent 50-ml *B. pseudomallei* cultures were grown for 24 h in 250-ml Erlenmeyer flasks shaken at 150 rpm, and growth curves were initiated by seeding fresh cultures to initial optical densities at 600 nm (OD_{600}) of 0.05. *B. pseudomallei* growth was monitored on an hourly basis both by viability counts as described previously (23) and by OD_{600} readings. The two methods gave similar results (see supplementary information at http://www.gis.a-star.edu.sg/internet/site/investigators.php?f = cv&user_id = 37), and an analysis of three replicate growth curves performed on different days confirmed the absence of significant day-to-day or batch variability (see supplementary information). To harvest sufficient RNA for each time point in the growth curve, we adopted a pooling approach, as institutional biosafety regulations prohibit large-volume growth of *B. pseudomallei*. Specifically, we generated a total of 138 separate 50-ml cultures grown as "batch clusters" of 16 to 18 flasks on multiple days. Each batch cluster of 16 to 18 culture flasks was derived from a single plate (LB) colony inoculated into a 25-ml starter culture shaken at 37°C at 150 rpm for 18 h. The starter culture was spun down at 3,500 rpm for 10 min, resuspended in 10 ml of 0.85 M saline (Oxoid Ltd., Basingstoke, Hampshire, United Kingdom), and spun again at 3,500 rpm for 5 min. The final 1-ml suspension was used to seed all flasks in the batch cluster to an OD_{600} of 0.05, corresponding to an average initial inoculum of 2.5×10^7 viable cells per ml. Cultures corresponding to the different batch clusters were then grown and harvested at the appropriate time points (see Fig. 1). The final expression profile data set comprises 47 composite time points sampled at 30-min intervals.

For *B. pseudomallei* 576 and *serC* mutant 4D6 growth, 5-ml TSB starter cultures were incubated for 15 h with shaking at 70 rpm. After centrifugation (3,000 rpm for 10 min) and washing with 1× phosphate-buffered saline, the bacterial pellets were used to initiate fresh TSB, CDM, or CDM–15 mM L-serine cultures (50 ml) at a starting OD_{600} of 0.05. All growth cultures were then shaken at 150 rpm, and hourly growth was monitored by OD_{600} readings.

DNA microarrays. Details of the *B. pseudomallei* DNA microarray used in the paper have been previously published (26) and are at www.omniarray.com/Bpm_Different_Strains/Supplemental. Briefly, the DNA microarray contains >8,000 probes printed in duplicate. These probes represent all 5,742 predicted genes in the *B. pseudomallei* K96243 genome (14) and also include >2,000 intergenic regions. Probes of 300 to 1,000 bp in length were PCR amplified and spotted in duplicate onto coated glass slides (Full Moon Biosystems Inc., Sunnyvale, CA).

***B. pseudomallei* RNA extraction and microarray hybridization.** Total RNA was isolated from bacterial pellets by using Trizol (Invitrogen Corporation, Carlsbad, California) and further purified using the Megaclear kit (Ambion, Inc., Austin, Texas). Samples were enriched for mRNA by using the MICROBExpress kit (Ambion, Inc., Austin, Texas) and hybridized to *B. pseudomallei* whole-genome microarrays using an indirect labeling strategy as previously described (27). Briefly, 1.5 μg of mRNA for each growth curve time point was reverse transcribed using random hexamer primers (Roche Diagnostics GmbH, Mannheim, Germany), Superscript II (Invitrogen, Carlsbad, CA), and a deoxynucleoside triphosphate mixture containing aminoallyl-dUTP (Sigma-Aldrich Co., St. Louis, MO). As a reference sample, we used mRNA isolated from a stationary-phase 18-h *B. pseudomallei* culture that was also labeled with aminoallyl-dUTP (Sigma-Aldrich Co., St. Louis, MO). The growth curve and reference samples were then labeled with Cy3 and Cy5 dye esters, respectively (Amersham Biosciences, UK Ltd., Buckinghamshire, United Kingdom). After removal of excess dyes, the labeled cDNAs were then hybridized onto the glass microarray using a hybridization mixture containing 1.25× SSC (1× SSC is 0.15 M NaCl plus 0.015 M sodium citrate), 0.08% sodium dodecyl sulfate (SDS), and elution buffer (QIAGEN GmbH, Hilden, Germany) for 16 h in a 65°C water bath. After hybridization, the slides were gently agitated in a solution of 2× SSC and 0.3% SDS at 55°C to dislodge the coverslips and dunked in a fresh solution of 2× SSC and 0.3% SDS at 55°C for 5 min. Slides were further dunked twice in 1× SSC at 55°C for 5 min each. Finally, the slides were dunked for 5 min in 0.2× SSC and dunked thrice in distilled water before being allowed to spin dry at 500 rpm for 20 min. The washed arrays were scanned using a Genepix scanner 4000B (Axon Instruments, Foster City, CA).

Data analysis. Raw microarray data was normalized using a LOWESS protocol (8). We selected 1,066 probes representing 974 distinct genes which both were reliably measured at more than two-thirds of all time points and demonstrated a >1.5-fold change in a minimum of two consecutive time points. Notably, although one biological replicate was used for each time point, we specifically selected genes exhibiting a >1.5-fold expression change in at least two consecutive time points; thus, each time point effectively serves as a "replicate" of adjacent points. For these selected genes, the missing values of their expression profiles were estimated using SVDImpute (45). We applied principal-component analysis on the mean-centered expression profiles of the selected genes to identify predominant gene expression patterns. The 10 most significant components, containing more than 95% of the variance, were used to reconstruct the gene expression data set, and k-means clustering (11) was then used to group the genes into 11 distinct groups, of which the top 9 were deemed the most biologically relevant. The results were visualized using Treeview software.

Functional annotations of growth-regulated genes (GRGs). The hypergeometric distribution was used to assess the significance of functional enrichments within each cluster based on genome-wide COG (clusters of orthologous groups) annotations. The COG database is accessible at http://www.ncbi.nlm.nih.gov/COG/new/.

Semiquantitative RT-PCR. cDNAs was generated from mRNA (1 μg/reaction) extracted from *B. pseudomallei* samples at the relevant time points by using random hexamer primers and a Becton Dickinson Clontech Advantage RT-for-PCR kit (Becton Dickinson, Franklin Lakes, New Jersey) according to the manufacturer's protocol. Semiquantitative PCR was performed on a MJ Research DNA engine Dyad Peltier thermocycler (Bio-Rad Laboratories, Hercules, California) in a 100-μl reaction volume, using 5 units of Platinum *Taq* DNA polymerase (Invitrogen, Carlsbad, California) in the presence of 200uM deoxynucleoside triphosphates, 2 mM $MgCl_2$, 10% (vol/vol) dimethyl sulfoxide, and 200 nM of each primer. The primers used are listed in the supplementary data at http://www.gis.a-star.edu.sg/internet/site/investigators.php?f = cv&user_id = 37. In each reverse transcription-PCR (RT-PCR) experiment, amplification of 16S rRNA was used as a positive and normalization control. For operon validation, we designed primers to the following adjacent gene pairs, where the forward primer was targeted to the first gene and the reverse primer to the second: BPSL1216/BPSL1217, BPSS0182/BPSS0183, BPSS1954/BPSS1955, and BPSL1468/BPSL1469.

Identification of *B. pseudomallei serC* mutants. To isolate *serC* mutants, we screened a previously described (2) bank of *B. pseudomallei* 576 transposon mutants. Briefly, wild-type *B. pseudomallei* 576 was transformed by electroporation (2.5 kV, 200 Ω, and 25 μF capacitance) using a Bio-Rad Gene Pulser II (Bio-Rad Laboratories Ltd., Hemel Hempstead, Herts, United Kingdom) with plasmid pUTminiTn5Km2, and transformed cells were selected on LB agar containing kanamycin (700 μg/ml). To ensure plasmid loss, randomly selected bacterial mutants were screened by PCR for the loss of nucleotide sequences

encoding the transposase enzyme necessary for transposon integration. No mutants that had the transposase gene sequence were identified, indicating loss of the suicide plasmid. Pools of transposon mutants were short-listed for their ability to grow on LB agar and inability to grow on minimal M9 medium. One of these mutants, 4D6, was confirmed to have an insertion in *serC*. Briefly, we used single-primer PCR to amplify DNA fragments adjacent to the transposon (2) in 4D6 genomic DNA, sequenced the amplified products, and queried the resultant sequences against the completed *B. pseudomallei* genome sequence by using BLAST. This analysis revealed the interrupted gene in 4D6 to be *serC*.

Virulence and vaccine assays. All investigations involving animals were carried out according to the requirements of the Animal (Scientific Procedures) Act of 1986. For virulence studies, we used age-matched (6-week-old) female BALB/c mice. We have previously shown that the median lethal doses (MLD) of *B. pseudomallei* 576 and K96243 by the intraperitoneal route in BALB/c mice are 80 and 100 CFU, respectively (2, 14). After challenge with viable *B. pseudomallei*, the infected animals were handled under biosafety level III containment conditions within a half-suit isolator, compliant with British standard BS5726. To establish the relative virulence of the *serC* mutant, we challenged six groups of five BALB/c mice with increasing doses of the *serC* mutant (10^3 to 10^8 CFU), monitored the infected mice for up to 5 weeks, and calculated the *serC* MLD by the method of Reed and Muench (32). For vaccination studies, we first infected animals with 10^5 CFU of the *serC* mutant, waited 5 weeks, and then challenged the animals with 1×10^4 CFU of either wild-type *B. pseudomallei* strain (K96243 or 576) and monitored the animals for survival as described above.

Chromosomal and operon analysis. The significance of biases in growth-regulated genes between the *B. pseudomallei* chromosomes was assessed using Fisher's exact test. Chromosomal clustering of growth-regulated genes was assessed using a moving window of ±3 genes and computing within each window the mean Pearson's correlation of gene expression by averaging all pairwise Pearson's correlations within the window. This distribution was compared against 10 randomly permuted data sets where the genomic order of the array probes was randomly scrambled. To compute enrichments of same-strand gene pairs, we performed bootstrapping assays where the number of observed same-strand gene pairs in the predicted operons was compared against random samples (with replacement) of 258 gene pairs in Chr 1 and 181 in Chr 2, across 10,000 repetitions. *P* values were calculated and plotted on a graph for both chromosomes (see supplementary information at http://www.gis.a-star.edu.sg/internet/site/investigators.php?f = cv&user_id = 37). To identify differences in intergenic length, the intergenic lengths associated with same-strand gene pairs in the predicted operons were compared against intergenic lengths in the entire genome by using a standard two-tailed *t* test.

Microarray data accession number. The complete microarray data set is available under GEO accession number GSE5495.

RESULTS

Expression profiling of the *B. pseudomallei* growth transcriptome. We compared multiple 24-h growth curves of *B. pseudomallei* and found that *B. pseudomallei* growth in rich medium was highly consistent, predictable, and reproducible (see supplementary information at http://www.gis.a-star.edu.sg/internet/site/investigators.php?f = cv&user_id = 37). Using a pooling approach (see Materials and Methods), we assembled a composite growth curve from multiple *B. pseudomallei* cultures sampled at 30-min intervals over 24 h (see Materials and Methods) (Fig. 1A). For each time point, bacterial mRNA was isolated and hybridized onto *B. pseudomallei* DNA microarrays containing >8,000 probes, including all 5,742 predicted genes in the *B. pseudomallei* genome and approximately 2000 intergenic regions. When an unsupervised hierarchical clustering algorithm was used to group the sample expression profiles with one another on the basis of their overall similarity, the samples separated into three distinct groups corresponding to early, log, and stationary phases, indicative of the biological distinctiveness of the three growth phases (see supplementary information). Using a combination of principal-component analysis and k-means clustering, we identified the nine most predominant patterns of gene expression and depicted these patterns as a red-green heat map (Fig. 1B). We observed that most, if not all, of the expression clusters were strongly associated with specific growth phases and transition points (i.e., early to log or log to stationary), which allowed us to define an operational set of "early" (E1 and E2), "log" (L1 to L4), and "stationary" (S1 to S3) clusters. To validate the microarray data by an alternative experimental method, we used semiquantitative PCR to investigate the expression patterns of 13 representative genes whose expression was broadly distributed throughout the time course but which otherwise were randomly selected. We found that there was excellent concordance between the PCR and microarray results (Fig. 1C). To reflect their association with the known growth phases, we henceforth refer to the genes in these clusters as GRGs.

Three points concerning the GRGs are worth noting. First, the expression clusters, ranging in size from 50 to 200 genes, are each expressed with highly distinct kinetic and temporal patterns. For example, some clusters were short lived with a rapid rise and fall of expression levels (e.g., cluster L1 at the transition from early to log phase), while other clusters were slower to rise and had prolonged expression plateaus (e.g., cluster S2, arising at mid-log phase and persisting throughout stationary phase). The temporal heterogeneity of these profiles suggests the existence of a tightly coordinated transcriptional process associated with *B. pseudomallei* growth. Second, the availability of a finely sampled time course allowed us to discern some clusters as being qualitatively distinct from others, which may have been missed if a coarser sampling approach had been used. For example, although clusters E1 and E2 are both expressed during early phase, the former is rapidly shut off at the transition from early to log phase, while the latter persists through the start of log phase. Similarly, the two log-phase clusters L2 and L3 share a common peak of expression at mid-log phase, but L2 displays a more prolonged and broader temporal profile than L3. Third, under the specific parameters used in our analysis, we identified 974 GRGs, suggesting that at least 17% of the *B. pseudomallei* genome is transcriptionally regulated during growth in rich medium. Taken collectively, these results demonstrate that the *B. pseudomallei* growth transcriptome is widespread and associated with a high level of coordination and regulation. We also note here that the two-color microarray format used in this study is suitable only for measuring relative expression changes. Thus, we are unable to comment either on the fraction of genes exhibiting constitutive but unaltered expression throughout the time course or on the fraction of genes that were not expressed under these in vitro conditions.

Biological coherence of expression clusters. Previous genome-wide growth studies of other microorganisms have suggested that genes with similar or related cellular functions are often coexpressed (4, 18). We asked if a similar phenomenon might also be observed in the *B. pseudomallei* growth transcriptome and if there were significant functional differences between the distinct expression clusters. As described below, we found that genes in the distinct expression clusters were indeed associated with highly related cellular functions. To perform this analysis, we first mapped the *B. pseudomallei* GRGs to their respective COG entities. The COG database is a public bioinformatic database (http://www.ncbi.nlm.nih.gov/COG) that groups protein sequences on the basis of phylogenetic similar-

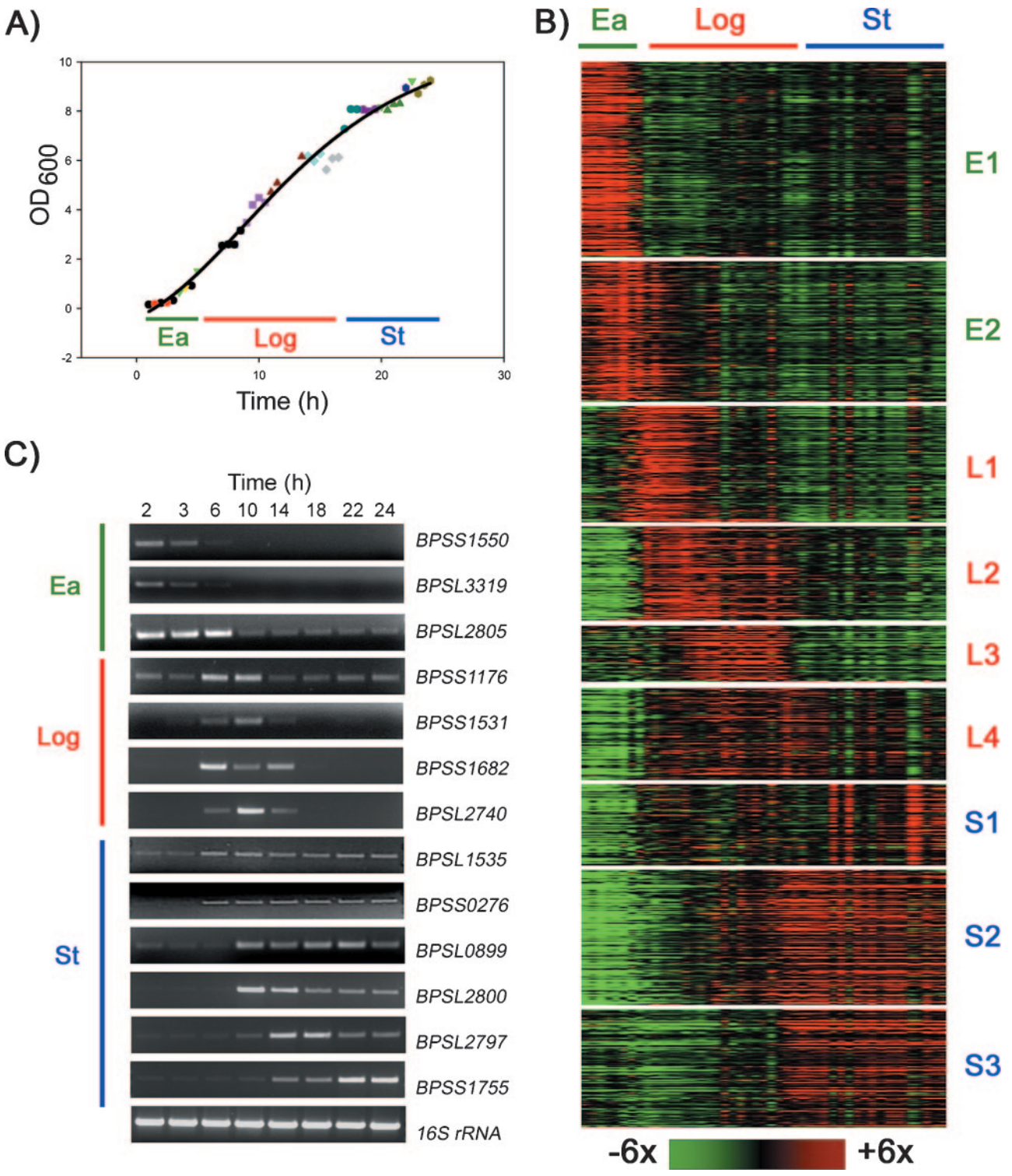

FIG. 1. Profiling of the *B. pseudomallei* growth transcriptome. (A) Composite growth curve of *B. pseudomallei* as a function of optical density (*y* axis) and time (*x* axis). Different-colored symbols represent samples from distinct batch clusters; for example, pink squares represent a batch cluster of 16 flasks harvested for time points 9 h to 10.5 h, and lime green inverted triangles represent another batch cluster of 14 flasks that were harvested for time points 3.5 h, 5 h, 20 h, and 22.5 h. Graph points represent individual time points used for subsequent expression profiling. Early (Ea), log, and stationary (St) phases are depicted. (B) Heat map of the *B. pseudomallei* growth transcriptome. Rows represent individual array probes, columns represent individual time points (30 min to 48 h), and distinct k-means clusters are shown as separate map blocks (e.g., E1 to S4, where E, L, and S represent early, log, and stationary phases, respectively). Red and green bars represent clusters of high and low gene expression levels, respectively. (C) Experimental validation of microarray data by semiquantitative PCR. Each row represents an individual *B. pseudomallei* gene, and columns represent gene expression levels, normalized against 16S rRNA expression (bottom row).

ity to various cellular functions, such as protein translation, DNA replication and transcription, nuclear structure, and defense mechanisms. We asked if specific COG functions might be significantly overrepresented in particular expression clusters and not others, based upon the hypergeometric distribution test (see Materials and Methods). Here we present a few clusters to illustrate this concept. Interested readers are referred to the supplementary information at http://www.gis.a-star.edu.sg/internet/site/investigators.php?f = cv&user_id = 37, where full lists of genes in each cluster are provided. In the following sections, the gene names ascribed to the GRGs are based largely upon their overall homology to genes of other bacterial species and should not be taken to imply that the genes represent true evolutionary orthologs.

(i) Cluster E1 (early phase, 1 h to 3.5 h). Cluster E1, a large cluster of 185 genes, exhibits a sharply defined pattern of high expression at early phase with a rapid shutoff upon entry into log phase. Many of the GRGs in this cluster are involved in processes essential for general biosynthesis, with a significant COG overrepresentation of genes involved in energy production and conversion (COG enrichment P value = 6.38×10^{-5}), protein translation ($P = 4.79 \times 10^{-24}$), and nucleotide transport and metabolism ($P = 0.0089$). Some examples include genes for energy production (NADP dehydrogenase I chain A and E; ATP synthases I, F,G, and H; and cytochrome oxidase subunits 1 and 2), DNA and nucleic acid (*dnaA*, *guaA*, and genes for thymidylate synthase, ribonucleoside reductase, and DNA polymerase III b chain), cofactors (*bioB*, *hemE*, *ribB*, *cobO*, and *pdxJ*), amino acids (*argC*, *glyA*, *hisB*, *hisJ*, *hisP*, *ilvC*, *ilvE*, and *ilvL*), and protein synthesis components (several 30S and 50S ribosomal proteins). The rapid expression of genes in this cluster may be triggered by the sudden availability of rich nutrients in the external medium, coupled with the introduction of the bacteria into a new environment of low population density.

(ii) Cluster E2 (early phase, 1 h to 6 h). Cluster E2, with 133 genes, has an expression pattern similar to that of E1 but is distinct from the latter in that E2 has a more prolonged shutoff period that continues into the initial period of log phase. Like E1, E2 also possesses a number of genes related to core biosynthetic pathways (see supplementary data 1 at http://www.gis.a-star.edu.sg/internet/site/investigators.php?f = cv&user_id = 37), but it is particularly prominent in genes related to fatty acid synthesis and lipid metabolism (*htrB*, *fabD*, *fabH*, and *plsC*). Another major distinctive feature of E2 not found in E1 is a significant enrichment of bacterial motility genes ($P = 9.87 \times 10^{-4}$), including genes for flagellar synthesis (*fliC*, *fliD*, and *fliM*), and chemotaxis (*cheY*, *cheR*, *motA*, and *motB*). We speculate that the expression of these early-phase motility genes may allow individual bacteria to maximize the use of available nutrients by migrating and spreading to separate nutrient-rich pockets before entering into a period of rapid cellular division, although further experimental work will be required to establish this. Notably, mutations in *fliC* have been shown to cause virulence attenuation in *B. pseudomallei* (7).

(iii) Cluster L1 (log phase, 3.5 h to 9 h). Cluster L1, with 110 genes, has an extremely sharp expression pattern coinciding with the transition period from early to log phase (3.5 h to 9 h). Genes in this cluster are associated with a broad set of processes, including amino acid catabolism (*arcB*, *arcC*, and *astE*), protein folding (*htpG*, *groEL*, and *groES2*), and secondary metabolic pathways (numerous nonribosomal peptide synthase/polyketide synthase genes) ($P = 0.0057$). One notable set of genes expressed during this period are those for components of the quorum-sensing (QS) machinery, including *N*-acyl homoserine lactone synthase and its cognate transcriptional activator protein (41, 46). QS is a process utilized by numerous bacterial species to relate bacterial population density to internal gene expression programs. The activation of QS genes in this cluster is consistent with the bacterial population being about to enter a period of exponential growth and division. Notably, QS has also recently been implicated in *B. pseudomallei* virulence (41, 46).

(iv) Cluster L2 (log phase, 4 to 14 h). Cluster L2, with 89 genes, is expressed only during log phase, with a rapid shutoff upon entry into stationary phase. Thus, this cluster is expressed at a period where the bacterial population is exponentially dividing. Possibly reflecting the large metabolic demands associated with exponential cell division, several genes in this cluster are involved in the biosynthesis, transport, and catabolism of secondary metabolites ($P = 2.15 \times 10^{-4}$) associated with carbon and energy metabolism (*fabH*, *aldH*, and succinyl coenzyme A:3-ketoacid-coenzyme A transferase subunit A and B genes), and they also include a number of stress-related protein genes (*katG* and *ahpD*). There are also a substantial number of genes involved in posttranslational processes, including genes for serine proteases (BPSL0808 and BPSS0962), collagenases (BPSS0827), and oligopeptidases (BPSS1175).

(v) Cluster S3 (stationary phase, 14 h to 24 h). Cluster S3, with 112 genes, is expressed at the onset of stationary phase and continues its high expression until the cessation of the growth curve. During this period, microbial cells switch from a period of rapid growth and expansion to a maintenance state in attempts to preserve the integrity of the bacterium amid a crowded and nutrient-poor environment and to seek out new nutrient sources. Besides a significant enrichment of amino acid transport and metabolism genes ($P = 0.0057$), we observed the expression of genes for several stress-related proteins (*sodB*, *sspA*, and *katE*), transport processes (*emrB*, *livG*, and *braG*), and a large set of transcriptional regulators and sensor proteins (*vsrD*, *hrpX*, *rpoD*, and *sdiA*).

Collectively, it can be seen that each of the expression clusters appears to be biologically coherent and related to distinct cellular functions. This may allow *B. pseudomallei* to optimally exploit its environment, from rapid growth to cellular maintenance.

Regulation of virulence genes in GRGs and identification of *serC* as a potential virulence factor. We next investigated if the expression of previously defined virulence genes in *B. pseudomallei* might be associated with any particular growth phase or transition point. Although the in vitro conditions used to generate the growth data are almost certainly different from those encountered by *B. pseudomallei* during the course of in vivo infection, we nevertheless observed a wide distribution of virulence GRG expression across all phases of the growth transcriptome. For example, in early phase we observed regulation of genes related to type II O-antigenic polysaccharide synthesis (*rmlB*), capsule production (*wzm* and *wbcC*), type III secretion (*prgK*), and flagella (*fliC*), while in log phase we observed regulation of type III secretion genes (*bopD* and

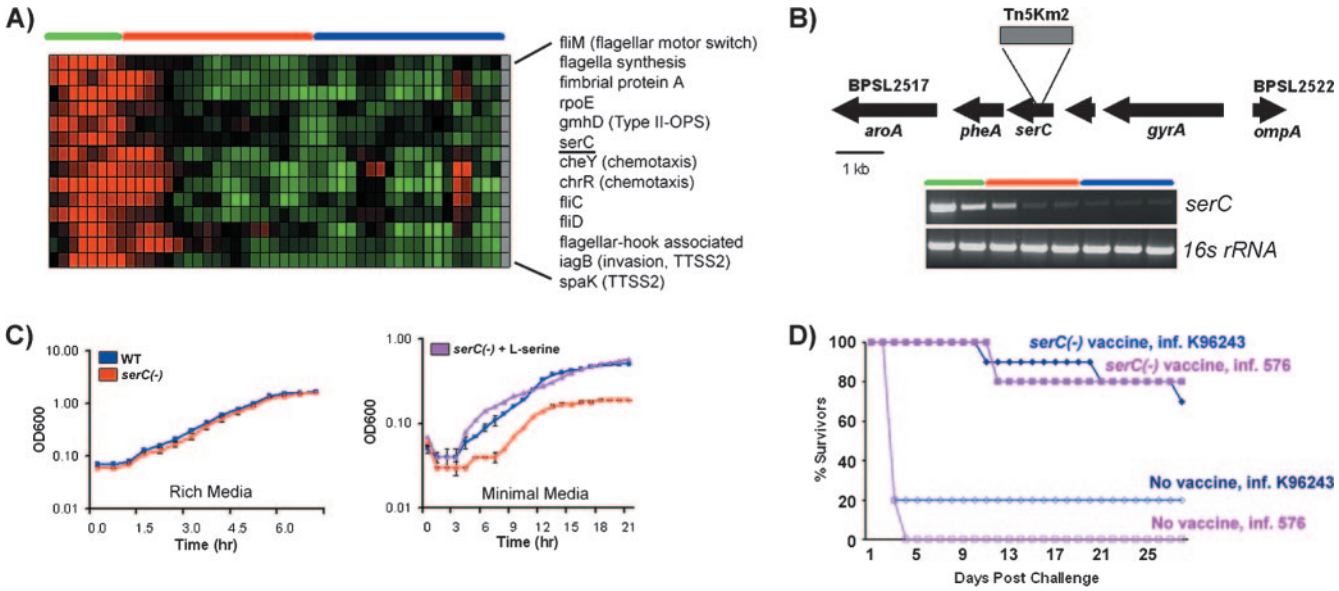

FIG. 2. Characterization of *serC* as a virulence gene. (A) Relationship of *serC* growth-regulated expression to expression of other virulence genes (see text for details). The serC gene is underlined. (B) Isolation of a *serC* mutant. The genome order of *serC* and neighboring genes, with insertion of an interrupting transposon, Tn*5*Km2, is shown. Also depicted is the confirmation of *serC* as an early-phase growth-regulated gene by semiquantitative PCR (see Fig. 1C). (C) Serine auxotrophy in *serC* mutants. Graphs represent growth curves of wild-type (WT) *B. pseudomallei* (blue) and *serC* mutants (red) in rich (left) and minimal (right) media. *serC* mutants exhibit slower growth in minimal medium, which can be rescued to wild-type levels by the addition of exogenous serine (pink). (D) Vaccination with *serC* mutants confers protection. Graphs represent rates of survival for animals either vaccinated with *serC* mutant *B. pseudomallei* (solid points) or not (open points) following subsequent challenge with different strains of *B. pseudomallei* (pink, strain 576; blue, strain K96243).

ipaD) and polysaccharide production genes (*rmlD* and *wcbE*). Many of these genes and their associated processes have been previously experimentally verified to be required for full expression of virulence in *B. pseudomallei* (7, 9, 31, 42). Given our findings in the previous section that many coexpressed genes appear to share similar functions, we then hypothesized that the microarray data could be used to identify new early-phase genes contributing to *B. pseudomallei* virulence. Specifically, we examined the E2 early-phase cluster and selected the gene *serC* by virtue of its coexpression with several known virulence genes, including *fliC*, *gmhD*, and *iagB* (Fig. 2A).

serC encodes a phosphoserine aminotransferase involved in serine and pyrioxidal 5′ phosphate biosynthesis. Our focus on *serC* was influenced by two key factors: its early-phase coexpression with other virulence genes and previous work by us and others showing that auxotrophic mutations in certain amino acid biosynthetic pathways are known to attenuate virulence in several pathogens (2, 38). However, not all amino acid auxotrophic mutants are attenuated (22), and to our knowledge a specific requirement for *serC* activity in virulence has not been previously reported for *B. pseudomallei* (see Discussion). To test the potential role of *serC* in *B. pseudomallei* virulence, we first performed semiquantitative PCR to validate *serC* as a specific early-phase gene. Confirming the microarray data, we found that the *serC* mRNA transcript level was high in early phase and declined to undetectable levels upon entry into log phase (Fig. 2B). Second, we proceeded to isolate a *B. pseudomallei* mutant deficient in *serC* activity. We reasoned that a *serC* disruption in *B. pseudomallei* should cause serine auxotrophy, similar to the case for *serC* mutations in other bacterial species (37). By screening a preexisting library of *B. pseudomallei* transposon mutants for their ability to grow on rich agar and inability to grow on minimal medium, we isolated one strain with a transposon insertion disrupting the *serC* gene (see Materials and Methods). Third, we characterized the growth kinetics of the *serC*-disrupted mutant. When cultured in rich medium, there was no significant difference between the growth rates of wild-type *B. pseudomallei* and *serC* mutants, indicating that a *serC* disruption does not cause a general growth defect (Fig. 2C, left panel). When cultured in minimal medium, *serC* mutants exhibited slower growth than wild-type *B. pseudomallei* during early phase, consistent with the gene expression of *serC* at this time Interestingly, the growth rates of *serC*-disrupted and wild-type *B. pseudomallei* strains were similar during log phase (compare the rates of increase curves during log phase in Fig. 2C, right panel), with the *serC* mutant ultimately reaching a lower final optical density at stationary phase (Fig. 2C, right panel). Fourth, to confirm that the growth defects of the mutant are specific to *serC* and not potential polar effects of the transposon on downstream genes, we performed biochemical complementation experiments by growing the mutant in minimal medium supplemented with serine. As can be seen from Fig. 2C, the addition of exogenous serine to the medium sufficed to restore the growth rate of the mutant to wild-type levels, indicating that the mutant growth defect is likely specific to a *serC* disruption. Taken collectively, these results indicate that disruptions in *serC* do indeed cause an early-phase growth defect in *B. pseudomallei*. However, it is worth noting that the *serC* mutant is still viable and capable of growth even in the total absence of all amino acids, indicating that *serC* is unlikely to be a completely essential gene.

To test the virulence of *serC B. pseudomallei* mutants, we

challenged BALB/c mice with intraperitoneal infections of *B. pseudomallei* and found that *serC* mutants exhibited a dramatic attenuation of virulence compared to the wild-type strain. Specifically, while the MLD of wild-type *B. pseudomallei* strain 576 was 100 CFU, the MLD of the *serC* mutant was 3.25×10^6 CFU, an attenuation of approximately ×40,000. (The MLD of wild-type strain K96243 was 262 CFU.) No deaths occurred in animals receiving the *serC* mutant at a dose of 1×10^6 CFU. At higher doses of 1×10^7 and 1×10^8 CFU, we observed 80% and 20% survival at the end of the experiment, respectively. This high level of attenuation is comparable to those of *B. pseudomallei* mutants that have been disrupted in major virulence factors, such as capsule formation (31). This result supports our hypothesis that *serC* may be an early-phase virulence gene in *B. pseudomallei*.

Vaccination with *serC* mutants offers cross-protection against multiple strains of wild-type *B. pseudomallei*. We then investigated whether prior vaccination of mice with *serC*-disrupted mutants might impart protection against subsequent challenges by wild-type *B. pseudomallei*. We introduced intraperitoneally a sublethal dose of the *serC* mutant into BALB/c mice. After 5 weeks, the mice were challenged with 100 times the MLD of either wild-type *B. pseudomallei* strain 576 (100 CFU) or K96243 (262 CFU). As can be seen in Fig. 2D, 80% of *serC*-vaccinated mice infected with strain 576 survived compared to the control vaccination, which was associated with 100% lethality. Similarly, higher levels of survival were observed in *serC*-vaccinated mice challenged with K96243 than in control vaccinated mice. To further investigate the pathology of survival, we characterized the morphologies and bacterial contents of spleens from vaccinated and unvaccinated K96243-infected mice. Spleens from the *serC*-vaccinated groups were found to be uninfected, and interestingly, spleens from the control group were all visibly enlarged and contained multiple abscesses, indicating the presence of a chronic infection (M. S.-Tyson, unpublished data). These results suggest that prior exposure of mice to *serC* mutants can indeed confer protection against subsequent challenges by wild-type *B. pseudomallei*.

Chromosomal biases and global mapping of potential operons. Finally, as a complementary approach to the gene-by-gene analysis, we also investigated whether the *B. pseudomallei* growth transcriptome might possess larger-scale genomic patterns not obviously discernible by focusing on single genes alone. Previous bioinformatic analysis has shown that *B. pseudomallei* chromosome 1 contains an overrepresentation of housekeeping and core metabolic genes compared to chromosome 2, suggesting that Chr 1 may represent the ancestral *Burkholderia* chromosome (14). We investigated whether similar chromosomal biases could be observed in the *B. pseudomallei* growth transcriptome as well. Surprisingly, we found that GRGs regulated in early phase were significantly biased towards Chr 1 ($P < 0.001$ by Fisher's exact test), while GRGs in stationary phase were biased towards Chr 2 ($P = 0.019$) (Fig. 3A). This finding is consistent with idea that the two chromosomes in *B. pseudomallei* are functionally partitioned: the GRGs on Chr 1 are expressed in early phase and are involved primarily in core biosynthetic and conserved metabolic functions, while the apparent "switch" in GRGs towards Chr 2 in stationary phase may suggest that the stationary-phase GRGs on this chromosome are likely to be preferentially involved in the execution of accessory functions required for survival and adaptation to species-specific environmental niches.

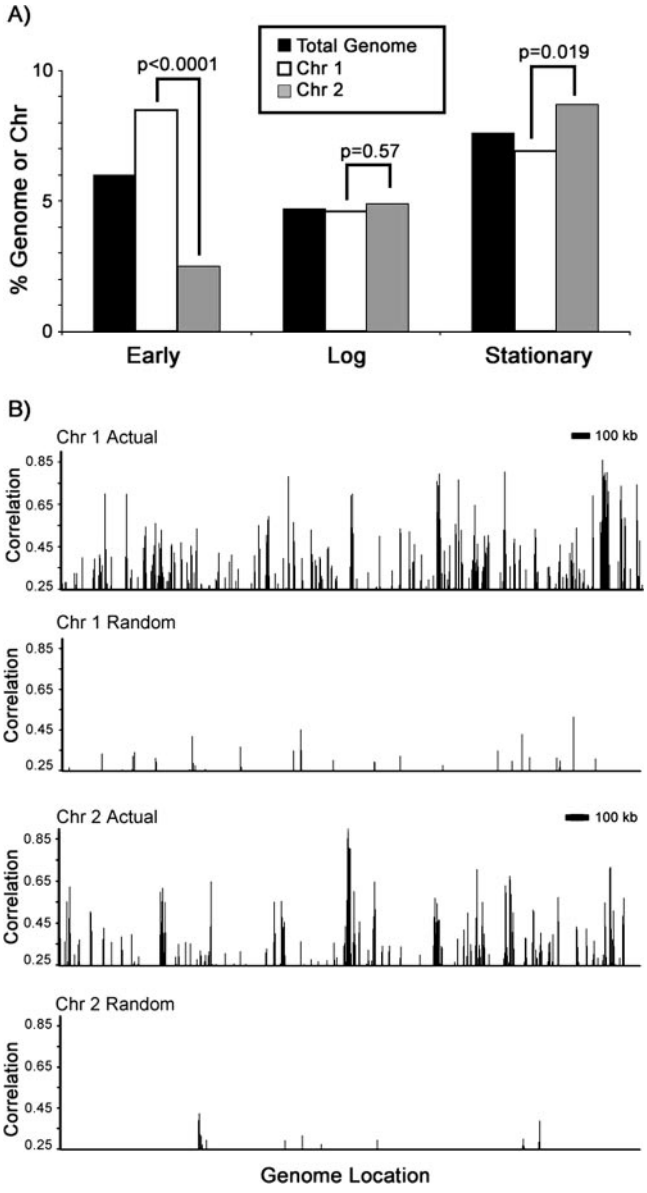

FIG. 3. Inter- and intrachromosomal clustering of growth-regulated genes. (A) Chromosomal biases in gene expression at early, log, and stationary phases. The *y* axis represents the total percentage of growth-regulated genes as a proportion of either the entire genome, chromosome 1, or chromosome 2. *P* values represent the significance of differences between the chromosomes, as assessed by Fisher's exact test. (B) Chromosomal clustering of growth-regulated genes. The *y* axis represents the expression correlation between all pairs of adjacent array probes for chromosome 1 and 2 (Chr 1 and 2 actual) or a randomized genome (Chr 1 and 2 random). The correlation value of 0.6 represents a cutoff FDR of 5%.

It is known that many genes in prokaryotes are transcribed as operons, where a common promoter controls multiple adjacent genes. With the exception of well-studied organisms such as *Escherichia coli* and *Bacillus subtilis*, surprisingly few data regarding operons are available for most bacterial species, including *B. pseudomallei*. Previous work has shown that gene

coexpression data can be effectively used as a basis for operon identification (35). To investigate whether the *B. pseudomallei* growth transcriptome could be used to generate a genomic map of putative *B. pseudomallei* operons, we first asked if there was a significant level of chromosomal clustering in the GRGs, which would be consistent with a high level of operon activity. By sliding a moving window across the entire *B. pseudomallei* genome, we computed the average correlation for every within-window array probe pair across the 24-h time series, where a high coefficient indicates the presence of chromosomally clustered coexpression (Fig. 3B). To determine the number of windows that might be assigned to the same operon by random chance (false discovery rate [FDR]), we compared the results of this analysis to a set of randomly permuted data where the genomic coordinates of the genes were scrambled (Fig. 3B shows typical randomized examples for Chr 1 and Chr 2). At every correlation coefficient cutoff, the numbers of clustered windows in the actual genome exceeded the randomized data. For example, at a window size of 5 and correlation coefficient cutoff of 0.5, there were 216 coexpression windows out of 3,133 total windows in the actual data for Chr 1, compared to 6 in the randomized data, thereby yielding an empirical FDR of 3.1% (see supplementary information at http://www.gis.a-star.edu.sg/internet/site/investigators.php?f = cv&user_id = 37). This result indicates that there is a significant level of chromosomal clustering of growth-regulated genes in the *B. pseudomallei* transcriptome, suggesting the existence of many potential operons that are activated during the process of *B. pseudomallei* growth. Given this result, we then proceeded to define a "gold standard" set of predicted *B. pseudomallei* operons for further analysis and validation (see below). Specifically, at a window size of 7 and correlation cutoff of 0.5, we defined a highly specific set of 462 chromosomally clustered GRGs, representing 96 potential operons in the *B. pseudomallei* genome. The FDR for this operon set is 0.43%, indicating that of the 96 operons, less than 1 is expected by random chance.

We then proceeded to computationally and experimentally validate the predicted *B. pseudomallei* operons by using a variety of methods previously used in other studies (5, 24, 44). First, we asked if genes inside a predicted operon had a preference to lie on the same strand, which would be consistent with an operon structure. Specifically, we compared the number of adjacent same-strand gene pairs in the list of 96 potential operons to the genome average (see supplementary information at http://www.gis.a-star.edu.sg/internet/site/investigators.php?f = cv&user_id = 37). In total, 90% (213/237 comparisons) and 80% (144/181 comparisons) of all possible adjacent gene pairs in the operon list were same-strand gene pairs for Chr 1 and Chr 2, respectively, which were significantly higher than the values for Chr 1 ($P < 0.0001$) and Chr 2 ($P = 0.088$ [here the significance is marginal]). Thus, genes within many of the predicted operons exhibit a strong tendency to lie on the same strand, consistent with their being true operons. Second, we asked if genes within the predicted operons were associated with significantly shorter intergenic lengths than the genome average (30), another hallmark of operons (24). Once again, we found that the average intergenic lengths of gene pairs in the predicted operon list were 142 bp and 228 bp for Chr 1 and Chr 2, respectively, significantly shorter than the genome averages of 225 bp for Chr 1 ($P = 2.262e{-}09$) and 279 bp for Chr 2 ($P = 0.01438$). Third, we asked if genes in the predicted operons tended to share similar functions, another common feature of operons. Indeed, we found that genes in the operons often shared similar cellular functions. For example, Chr 1 contains a large set of contiguous ribosomal protein genes (BPSL3193 to BPSL3225) and genes related to phenylacetic acid degradation (BPSL3230 to BPSL3234) and ATP synthesis (BPSL3395-BPSL3401), while Chr 2 contains operons relating to benzoate degradation (BPSS0042 to BPSS0048), nitrogen metabolism (BPSS1157 to BPSS1160), and type III secretion (BPSS1529 to BPSS1534). Fourth, to confirm that genes in a predicted operon were expressed as a common transcript, we selected four predicted operons (BPSL1215 to BPSL1217, BPSL1467 to BPSL1469, BPSS0181 to BPSS0183, and BPSS1954 to BPSS1956) for experimental validation. For each operon, we chose two genes and designed PCR primers where the forward primer was targeted to the first gene and the reverse primer was targeted to the second gene. When applied in an RT-PCR experiment, the presence of a discrete band at the expected size indicates that the selected genes, as well as their corresponding intergenic regions, are likely to be expressed as part of the same mRNA transcript. For all four regions, the RT-PCR experiment confirmed their expression as part of a common transcriptional unit, supporting their predicted status as operons (see supplementary information at http://www.gis.a-star.edu.sg/internet/site/investigators.php?f = cv&user_id = 37). Thus, based on multiple criteria that are largely independent of gene coexpression, the genes in the operon list are likely to represent true operons. The list of putative operons defined in this study represents the first database of operons in *B. pseudomallei*, and a complete list is provided in the supplementary information.

In addition to operons, we also note that some of the chromosomally clustered GRGs were suggestive of a more complex regulation. For example, BPSL1867 to BPSL1870 is a four-gene coexpression cluster where the first two member genes reside on the positive strand (positive) but the last two members reside on the negative strand, suggesting that their coexpression may arise from either the activation of two separate promoters (another example can be found in BPSL2456 to BPSL2457) or transcriptional readthrough. Further work will be required to unravel the mechanistic cause of such complex coexpression events.

DISCUSSION

In this report, we have described for the first time a genome-wide survey of growth-regulated gene expression in *B. pseudomallei*, the causative agent of melioidosis. Our results indicate that a sizeable proportion of the *B. pseudomallei* genome (at least 17%) is regulated during growth, which is manifested primarily as discrete waves of functionally coherent gene expression that are tightly associated with distinct growth phases and transition points. One notable aspect of our study was the use of a fine-scale sampling approach, which allowed us to identify closely related gene expression clusters as being distinct from one another (e.g., clusters E1/E2 and L2/L3). With the availability of this *B. pseudomallei* transcriptome map, a subsequent challenge will be to identify the specific *cis*- and *trans*-acting factors that are responsible for temporally control-

ling and regulating these highly coordinated waves of gene expression. At present, this is a formidable task, as very few transcription factors and their downstream targets in *B. pseudomallei* have been characterized (17, 41). Nevertheless, the data provided by our study represent an essential first step for subsequent in-depth transcriptional analysis, including gene expression network reconstruction or regulatory motif identification. The information in this report should thus prove valuable not only to the melioidosis research community but also to other microbial researchers, particularly since homologs of the *B. pseudomallei* GRGs can be found in many other bacterial species.

On an individual gene level, GRGs in an expression cluster tended to share similar cellular functions, with basic core processes such as amino acid synthesis and energy production occurring in early phase and secondary metabolic and accessory functions being activated during the stationary-phase period. Notably, previous genome-wide growth studies with other microorganisms have suggested the presence of a "just-in-time" manufacturing strategy, which may represent a general mechanism employed by microbial species to optimize and allocate cellular resources only when needed (4, 18). Although further experimental testing is required to address whether the "just-in-time" strategy is generally applicable to *B. pseudomallei*, there are certain hints that this phenomenon may also be present in the *B. pseudomallei* growth transcriptome. For example, we observed activation of several quorum-sensing machineries just prior to the population initiating exponential growth (cluster L1), which would coincide with a period of rapid expansion where population numbers need to be tightly monitored. Furthermore, our discovery in this study that *serC* mutants have an early-phase growth defect, which coincides with the time of expression of this gene, may also support the presence of a just-in-time approach. Interestingly, although the bacteria in this study were cultured in rich medium where nutrients are abundant, we nevertheless observed up-regulation of several core biosynthetic genes during early phase. Such GRGs may represent a "hard-wired" transcriptional circuitry that is activated regardless of external nutrient status during early phase. Alternatively, these genes may be responding to other environmental cues, such as fluctuations in population density. An important avenue of future research will be to define the extent to which the GRGs are directly dependent on external environmental cues or whether they are initiated as part of a "hard-wired" transcriptional cascade. Furthermore, although we have focused on up-regulated genes in this study, it is quite possible that the down-regulation of certain genes at specific time points may also be important for microbial physiology and pathogenicity. For example, down-regulation of the two type III secretion components BPSS1526 and BPSS1542 during log and stationary phases may be important for proper assembly and functioning of the *B. pseudomallei* type III secretion apparatus. This is another area that deserves further study.

A major finding in our study was the identification of *serC* as a potential virulence gene in *B. pseudomallei*. We chose the *serC* gene based on several criteria. First, we specifically focused on early-phase genes, as previous reports investigating microbial growth and virulence have concentrated on later time points such as stationary phase and the transition from log to stationary phase (20, 39, 48). Second, we selected the E2 early-phase expression cluster, since it contained several coexpressed genes previously demonstrated to be important for *B. pseudomallei* virulence. Third, given our previous studies relating auxotrophic mutants to virulence, we considered E2 cluster genes likely to produce auxotrophic phenotypes when disrupted. Fourth, among these candidates we chose *serC* due its novelty (see below) and not other genes in amino acid pathways shown previously to regulate virulence, including branched-chain amino acid (*BPSL1201* [*leuA*], 2-isopropylmalate synthase), arginine (BPSL1742 [*arcD*]), and cysteine (BPSL2507 [*cysM*], cysteine synthase) biosynthesis (33, 36). Although a search of the PubMed/Medline literature does identify a few prior studies suggesting an apparent relationship between serine auxotrophy and virulence, these connections are largely indirect and not well established. For example, Van Der Walt and Greeff (47) described using a *serC* mutant of *Salmonella enterica* serovar Typhimurium as a vaccine strain; however, the attenuation of virulence in this strain was attributed to curing of the *S. enterica* serovar Typhimurium virulence plasmid rather than the specific loss of *serC* activity. Similarly, Hoiseth and Stocker (13) reported that *aroA serC* strains of *S. enterica* serovar Typhimurium are serine auxotrophs and show attenuated virulence, but it is not clear if the virulence attenuation was due to loss of *serC* or *aroA* activity. To our knowledge, our study represents the first time that a requirement for *serC* has been shown for virulence in any member of the *Burkholderia* family. Although the mechanistic basis of virulence attenuation in the *serC* mutant currently remains unclear, we believe that there are at least two possibilities, which we refer to as the "nutritional" and "regulatory" models. The nutritional model posits that *serC* acts primarily as a housekeeping gene generally required for *B. pseudomallei* growth and that the observed virulence attenuation in *serC* mutants is the simple result of the *serC* mutants failing to grow in the mice or being rapidly cleared by the immune system. In this model, *serC* would still be technically classified as a virulence gene, but in reality its identification would provide little information regarding the specifics of *B. pseudomallei* pathogenesis. Although we did not directly measure the in vivo growth rates of *serC* mutants in this study, we believe that the nutritional model is unlikely to completely explain the *serC* virulence attenuation for the following reasons. First, our in vitro experiments indicate that *serC* mutants are unlikely to exhibit a general growth defect as expected for a general housekeeping gene. Specifically, the growth curves of wild-type and *serC* strains in rich medium are essentially identical, and *serC* mutants are capable of growing even in minimal medium where all amino acids are absent. Second, the growth defect of the *serC* mutant in minimal medium does not appear to be a generalized effect but is instead largely specific to early phase and can be completely restored by the addition of exogenous serine. Third, chemical analysis of human serum suggests that the levels of exogenous free serine in human serum are unlikely to be limiting for *serC* mutant growth (19, 29). For these reasons, we currently favor the regulatory model, which posits that *serC* may not simply act as a general housekeeping gene but may also be involved in the synthesis of components specifically required for *B. pseudomallei* virulence. As an analogy, mutations in the aromatic acid synthesis pathway are thought to

cause virulence attenuation due to decreased levels of enterobactin, which is required for iron scavenging by many pathogens (10). Clearly, unraveling the mechanism behind the virulence attenuation of the *serC* mutants is an important area of future study.

We also investigated whether *serC* mutants, due to their dramatically attenuated virulence, might also function as a potential vaccine to confer protection against challenges by wild-type *B. pseudomallei*. We have also previously shown that protection can be conferred by vaccinating mice with another auxotroph of *B. pseudomallei*, which is mutated in the *ilvI* gene, which encodes the large subunit of the acetolactate synthase enzyme (2). We found that prior immunization of mice with a sublethal dose of *serC* mutant *B. pseudomallei* was able to confer protection against subsequent challenges by different strains of *B. pseudomallei*. Protection against at least two different strains of *B. pseudomallei* was provided, although the levels of protection conferred were slightly different. This could be due to different intrinsic potencies of virulence between the *B. pseudomallei* strains and possibly to variations in their surface lipopolysaccharides (1). A potentially interesting area of future research will be to determine if such a combined auxotroph may prove clinically useful in the development of an actual *B. pseudomallei* vaccine, although additional genetic manipulation of these attenuated strains, perhaps through a *serC ilvI* compound mutation, will undoubtedly be required to confer an irreversibly attenuated virulence phenotype. In addition, it will be critical to study the specific host response to the *serC* vaccine and to determine if the conferred protection is short-term or long lasting.

In conclusion, we have described in this report a genome-wide characterization of the *B. pseudomallei* growth transcriptome. Our results suggest that *B. pseudomallei* utilizes an extensive and highly coordinated transcriptional structure to maximize available nutrients and that the processes of virulence and growth are tightly integrated in this species. As the data in this data set are extremely rich, it is likely that further analyses of these data, using more sophisticated algorithms and targeted hypotheses, will be fruitful avenues for more insights into pathogen discovery and behavior. As bacterial growth processes are conserved across many different species, it is possible that many of the findings in our study may find broad applicability to other important pathogens.

ACKNOWLEDGMENTS

This work was funded by internal grants from GIS and DMERI to P.T. and from DSTL to R.W.T.

We thank Edison Liu and Lionel Lee for their advice and encouragement.

REFERENCES

1. **Anuntagool, N., P. Intachote, V. Wuthiekanun, N. J. White, and S. Sirisinha.** 1998. Lipopolysaccharide from nonvirulent Ara$^+$ *Burkholderia pseudomallei* isolates is immunologically indistinguishable from lipopolysaccharide from virulent Ara$^-$ clinical isolates. Clin. Diagn. Lab. Immunol. **5:**225–229.
2. **Atkins, T., R. G. Prior, K. Mack, P. Russell, M. Nelson, P. C. F. Oyston, G. Dougan, and R. W. Titball.** 2002. A mutant of *Burkholderia pseudomallei*, auxotrophic in the branched-chain amino acid biosynthetic pathway, is attenuated and protective in a murine model of melioidosis. Infect. Immun. **70:**5290–5294.
3. **Bachman, M. A., and M. S. Swanson.** 2004. Genetic evidence that *Legionella pneumophila* RpoS modulates expression of the transmission phenotype in both the exponential phase and the stationary phase. Infect. Immun. **72:**2468–2476.
4. **Bozdech, Z., M. Llinas, B. L. Pulliam, E. D. Wong, J. Zhu, and J. L. DeRisi.** 2003. The transcriptome of the intraerythrocytic developmental cycle of *Plasmodium falciparum*. PLoS. Biol. **1:**E5.
5. **Chen, X., Z. Su, P. Dam, B. Palenik, Y. Xu, and T. Jiang.** 2004. Operon prediction by comparative genomics: an application to the *Synechococcus* sp. WH8102 genome. Nucleic Acids Res. **32:**2147–2157.
6. **Cheng, A. C., and B. J. Currie.** 2005. Melioidosis: epidemiology, pathophysiology, and management. Clin. Microbiol. Rev. **18:**383–416.
7. **Chua, K. L., Y. Y. Chan, and Y. H. Gan.** 2003. Flagella are virulence determinants of *Burkholderia pseudomallei*. Infect. Immun. **71:**1622–1629.
8. **Cleveland, W. S.** 1979. Robust locally weighted regression and smoothing scatterplots. J. Am. Stat. Assoc. **74:**829–836.
9. **DeShazer, D., P. J. Brett, and D. E. Woods.** 1998. The type II O-antigenic polysaccharide moiety of *Burkholderia pseudomallei* lipopolysaccharide is required for serum resistance and virulence. Mol. Microbiol. **30:**1081–1100.
10. **Edwards, M. F., and B. A. Stocker.** 1988. Construction of Δ*aroA his* Δ*pur* strains of *Salmonella typhi*. J. Bacteriol. **170:**3991–3995.
11. **Eisen, M. B., P. T. Spellman, P. O. Brown, and D. Botstein.** 1998. Cluster analysis and display of genome-wide expression patterns. Proc. Natl. Acad. Sci. USA **95:**14863–14868.
12. **Ha, U., and S. Jin.** 2001. Growth phase-dependent invasion of *Pseudomonas aeruginosa* and its survival within HeLa cells. Infect. Immun. **69:**4398–4406.
13. **Hoiseth, S. K., and B. A. Stocker.** 1985. Genes *aroA* and *serC* of *Salmonella typhimurium* constitute an operon. J. Bacteriol. **163:**355–361.
14. **Holden, M. T., R. W. Titball, S. J. Peacock, A. M. Cerdeno-Tarraga, T. Atkins, L. C. Crossman, T. Pitt, C. Churcher, K. Mungall, S. D. Bentley, M. Sebaihia, N. R. Thomson, N. Bason, I. R. Beacham, K. Brooks, K. A. Brown, N. F. Brown, G. L. Challis, I. Cherevach, T. Chillingworth, A. Cronin, B. Crossett, P. Davis, D. DeShazer, T. Feltwell, A. Fraser, Z. Hance, H. Hauser, S. Holroyd, K. Jagels, K. E. Keith, M. Maddison, S. Moule, C. Price, M. A. Quail, E. Rabbinowitsch, K. Rutherford, M. Sanders, M. Simmonds, S. Songsivilai, K. Stevens, S. Tumapa, M. Vesaratchavest, S. Whitehead, C. Yeats, B. G. Barrell, P. C. Oyston, and J. Parkhill.** 2004. Genomic plasticity of the causative agent of melioidosis, Burkholderia pseudomallei. Proc. Natl. Acad. Sci. USA **101:**14240–14245.
15. **Hsueh, P. R., L. J. Teng, L. N. Lee, C. J. Yu, P. C. Yang, S. W. Ho, and K. T. Luh.** 2001. Melioidosis: an emerging infection in Taiwan? Emerg. Infect. Dis. **7:**428–433.
16. **Huang, J., C.-J. Lih, K.-H. Pan, and S. N. Cohen.** 2001. Global analysis of growth phase responsive gene expression and regulation of antibiotic biosynthetic pathways in *Streptomyces coelicolor* using DNA microarrays. Genes Dev. **15:**3183–3192.
17. **Korbsrisate, S., M. Vanaporn, P. Kerdsuk, W. Kespichayawattana, P. Vattanaviboon, P. Kiatpapan, and G. Lertmemongkolchai.** 2005. The *Burkholderia pseudomallei RpoE* (AlgU) operon is involved in environmental stress tolerance and biofilm formation. FEMS Microbiol. Lett. **15:**252:243–249.
18. **Laub, M. T., H. H. McAdams, T. Feldblyum, C. M. Fraser, and L. Shapiro.** 2000. Global analysis of the genetic network controlling a bacterial cell cycle. Science **290:**2144–2148.
19. **Lehmann, M., M. Huonker, F. Dimeo, N. Heinz, U. Gastmann, N. Treis, J. M. Steinacker, J. Keul, R. Kajewski, and D. Haussinger.** 1995. Serum amino acid concentrations in nine athletes before and after the 1993 Colmar ultra triathlon. Int. J. Sports Med. **16:**155–159.
20. **Liu, H., N. H. Bergman, B. Thomason, S. Shallom, A. Hazen, J. Crossno, D. A. Rasko, J. Ravel, T. D. Read, S. N. Peterson, J. Yates III, and P. C. Hanna.** 2004. Formation and composition of the *Bacillus anthracis* endospore. J. Bacteriol. **186:**164–178.
21. **Lundberg, U., U. Vinatzer, D. Berdnik, A. von Gabain, and M. Baccarini.** 1999. Growth phase-regulated induction of *Salmonella*-induced macrophage apoptosis correlates with transient expression of SPI-1 genes. J. Bacteriol. **181:**3433–3437.
22. **Marquis, H., H. G. Bouwer, D. J. Hinrichs, and D. A. Portnoy.** 1993. Intracytoplasmic growth and virulence of *Listeria monocytogenes* auxotrophic mutants. Infect. Immun. **61:**3756–3760.
23. **Miles, A. A., S. S. Misra, and J. O. Irwin.** 1938. The estimation of bactericidal power of blood. J. Hyg. **38:**733–749.
24. **Moreno-Hagelsieb, G., and J. Collado-Vides.** 2002. A powerful non-homology method for the prediction of operons in prokaryotes. Bioinformatics **18**(Suppl. 1)**:**S329–S336.
25. **Nicholson, T. L., L. Olinger, K. Chong, G. Schoolnik, and R. S. Stephens.** 2003. Global stage-specific gene regulation during the developmental cycle of *Chlamydia trachomatis*. J. Bacteriol. **185:**3179–3189.
26. **Ong, C., C. H. Ooi, D. Wang, H. Chong, K. C. Ng, F. Rodrigues, M. A. Lee, and P. Tan.** 2004. Patterns of large-scale genomic variation in virulent and avirulent *Burkholderia* species. Genome Res. **14:**2295–2307.
27. **Ou, K., C. Ong, S. Y. Koh, F. Rodrigues, S. H. Sim, D. Wong, C. H. Ooi, K. C. Ng, H. Jikuya, C. C. Yau, S. Y. Soon, D. Kesuma, M. A. Lee, and P. Tan.** 2005. Integrative genomic, transcriptional, and proteomic diversity in natural isolates of the human pathogen *Burkholderia pseudomallei*. J. Bacteriol. **187:**4276–4285.
28. **Peng, X., R. K. Karuturi, L. D. Miller, K. Lin, Y. Jia, P. Kondu, L. Wang,**

L. S. Wong, E. T. Liu, M. K. Balasubramanian, and J. Liu. 2005. Identification of cell cycle-regulated genes in fission yeast. Mol. Biol. Cell **16:**1026–1042.
29. **Pitkanen, H. T., S. S. Oja, K. Kemppainen, J. M. Seppa, and A. A. Mero.** 2003. Serum amino acid concentrations in aging men and women. Amino Acids **24:**413–421.
30. **Price, M. N., K. H. Huang, E. J. Alm, and A. P. Arkin.** 2005. A novel method for accurate operon predictions in all sequenced prokaryotes. Nucleic Acids Res. **33:**880–892.
31. **Reckseidler, S. L., D. DeShazer, P. A. Sokol, and D. E. Woods.** 2001. Detection of bacterial virulence genes by subtractive hybridization: identification of capsular polysaccharide of *Burkholderia pseudomallei* as a major virulence determinant. Infect. Immun. **69:**34–44.
32. **Reed, L. J., and H. Muench.** 1938. A simple method of estimating 50 percent end-points. Am. J. Hyg. **27:**493–497.
33. **Rhodes, J. C., and D. H. Howard.** 1980. Isolation and characterization of arginine auxotrophs of *Cryptococcus neoformans*. Infect. Immun. **27:**910–914.
34. **Rolim, D. B.** 2005. Melioidosis, northeastern Brazil. Emerg. Infect. Dis. **11:**1458–1460.
35. **Sabatti, C., L. Rohlin, M. K. Oh, and J. C. Liao.** 2002. Co-expression pattern from DNA microarray experiments as a tool for operon prediction. Nucleic Acids Res. **30:**2886–2893.
36. **Scully, L. R., and M. J. Bidochka, M. J.** 2006. A cysteine/methionine auxotroph of the opportunistic fungus *Aspergillus flavus* is associated with host-range restriction: a model for emerging diseases. Microbiology **152:**223–232.
37. **Shimizu, S., and W. B. Dempsey.** 1978. 3-Hydroxypyruvate substitutes for pyridoxine in *serC* mutants of *Escherichia coli* K-12. J. Bacteriol. **134:**944–949.
38. **Smith, D. A., T. Parish, N. G. Stoker, and G. J. Bancroft.** 2001. Characterization of auxotrophic mutants of *Mycobacterium tuberculosis* and their potential as vaccine candidates. Infect. Immun. **69:**1142–1150.
39. **Snyder, J. A., B. J. Haugen, E. L. Buckles, C. V. Lockatell, D. E. Johnson, M. S. Donnenberg, R. A. Welch, and H. L. T. Mobley.** 2004. Transcriptome of uropathogenic *Escherichia coli* during urinary tract infection. Infect. Immun. **72:**6373–6381.
40. **Song, M., H.-J. Kim, E. Y. Kim, M. Shin, H. C. Lee, Y. Hong, J. H. Rhee, H. Yoon, S. Ryu, S. Lim, and H. E. Choy.** 2004. ppGpp-dependent stationary phase induction of genes on *Salmonella* pathogenicity island 1. J. Biol. Chem. **279:**34183–34190.
41. **Song, Y., C. Xie, Y.-M. Ong, Y.-H. Gan, and K.-L. Chua.** 2005. The BpsIR quorum-sensing system of *Burkholderia pseudomallei*. J. Bacteriol. **187:**785–790.
42. **Stevens, M. P., A. Friebel, L. A. Taylor, M. W. Wood, P. J. Brown, W.-D. Hardt, and E. E. Galyov.** 2003. A *Burkholderia pseudomallei* type III secreted protein, BopE, facilitates bacterial invasion of epithelial cells and exhibits guanine nucleotide exchange factor activity. J. Bacteriol. **185:**4992–4996.
43. **Thompson, L. J., D. S. Merrell, B. A. Neilan, H. Mitchell, A. Lee, and S. Falkow.** 2003. Gene expression profiling of *Helicobacter pylori* reveals a growth-phase-dependent switch in virulence gene expression. Infect. Immun. **71:**2643–2655.
44. **Tjaden, B., R. M. Saxena, S. Stolyar, D. R. Haynor, E. Kolker, and C. Rosenow, C.** 2002. Transcriptome analysis of *Escherichia coli* using high-density oligonucleotide probe arrays. Nucleic Acids Res. **30:**3732–3738.
45. **Troyanskaya, O., M. Cantor, G. Sherlock, P. Brown, T. Hastie, R. Tibshirani, D. Botstein, and R. B. Altman.** 2001. Missing value estimation methods for DNA microarrays. Bioinformatics **17:**520–525.
46. **Ulrich, R. L., D. DeShazer, E. E. Brueggemann, H. B. Hines, P. C. Oyston, and J. A. Jeddeloh.** 2004. Role of quorum sensing in the pathogenicity of *Burkholderia pseudomallei*. J. Med. Microbiol. **53:**1053–1064.
47. **Van Der Walt, M. L., and A. S. Greeff.** 1998. The production of an auxotrophic marked, plasmid-cured *Salmonella ser. Typhimurium* as a live attenuated vaccine. Onderstepoort J. Vet. Res. **65:**213–220.
48. **Wagner, V. E., D. Bushnell, L. Passador, A. I. Brooks, and B. H. Iglewski.** 2003. Microarray analysis of *Pseudomonas aeruginosa* quorum-sensing regulons: effects of growth phase and environment. J. Bacteriol. **185:**2080–2095.